

# A Compact Wide-Band Array Antenna for Ka-Band Applications

Pavada Santosh<sup>1</sup>, P. Ramesh<sup>2</sup>, Chitambara Rao Karedla<sup>3,\*</sup>, K. S. Chakradhar<sup>4</sup>, M. Lakshmunaidu<sup>5</sup>,  
and Harihara Santosh Dadi<sup>3</sup>

<sup>1</sup>Department of Electronics and Computer Engineering, Vignan's Institute of Information Technology, Duvvada, Visakhapatnam, AP, India

<sup>2</sup>Department of Electronics and Communication Engineering, Sri Indu College of Engineering and Technology, Sheriguda, Hyderabad, Telangana, India

<sup>3</sup>Department of Electronics and Communication Engineering, Aditya Institute of Technology and Management, Tekkali, Srikakulam, AP, India

<sup>4</sup>Department of Electronics and Communication Engineering, Mohan Babu University, Tirupati, India

<sup>5</sup>Department of Electronics and Communication Engineering, Koneru Lakshmaiah Education Foundation, Vaddeswaram, Guntur, AP, India

Email: santoshpavada@vignaniit.edu.in (P.S.); drpramesh87@gmail.com (P.R.); rao.chiddubabu@gmail.com (C.R.K.); chakradharec@gmail.com (K.S.C); laxman.naidu@gmail.com (M.L.); dhhsantosh@gmail.com (H.S.D.);

\*Corresponding author

**Abstract**—Ka-band frequencies are used in military aircraft, space telescopes, high-resolution, close-range targeting radars, commercial wireless point-to-point microwave communication systems, systems that measure vehicle speed, and satellite communications these days. For Ka-Band applications, it is very difficult to design an antenna and also a challenging task to obtain a sufficient gain, reflection coefficient, and Voltage Standing Wave Ratio (VSWR) because Ka-Band frequencies are very large. At these frequencies, so many issues will occur, like coupling, bandwidth, and sidelobe. In this work, a new design concept of a compact, wide-band, 10-element array antenna has been proposed for Ka-band (26 GHz–40 GHz) applications based on the non-uniform structure with non-uniform spacing between the patches. The proposed antenna is implemented on a  $31.3 \times 10.37 \times 0.787$  mm<sup>3</sup> RT duroid 5880 substrates with a relative dielectric constant of  $r = 2.2$  and a loss tangent of 0.0009. The proposed antenna is simulated for essential parameters like reflection coefficient, Voltage Standing Wave Ratio (VSWR), and gain. Following the simulation, fabricate and measure the antenna for the same essential parameters. At the end, the simulated and measured parameters are compared for the validation of an antenna to work at Ka-band frequencies. Based on the comparison, the proposed antenna yields better results, like a reflection coefficient less than  $-10$  dB,  $VSWR < 2$ , and a peak gain of 12.2 dBi. In addition, for the proposed antenna, a wide bandwidth of 16.75 GHz is achieved in the frequency range of 22 GHz to 38.75 GHz.

**Keywords**—array antenna, inset feed, Ka-Band, rectangular microstrip patch antenna

## I. INTRODUCTION

A lot of research has been done on the Ka-Band mm Wave frequency spectrum because of its possible application in 5G networks. Increasing the frequency of the Ka-band from 26 GHz to 40 GHz results in less attenuation and absorption by the atmosphere. Based on the metasurface Luneburg lens, a small millimetre wave antenna operating at 28 GHz has been developed for Ka-band 5G applications. A peak gain of 7.9 dBi and a return loss of less than  $-10$  dB have been attained by the developed antenna [1]. At Ka-Band, a patch antenna has been suggested for 5G applications. The antenna operates with a broad bandwidth of 1.40 GHz and a high gain of 8.10 dB at 38.10 GHz. The suggested antenna has a gain fluctuation of 0.30 dB and a high F/B ratio of 16.27 dB. [2]. A quad-element Multiple Input Multiple Output (MIMO) antenna intended for multiband applications, including a large section of the Ku band (12.4–15.5 GHz), the X band (8–12.4 GHz), and the C band (4–8 GHz). The two mm-wave bands it covers are 26.4–34.3 GHz and 36.1–48.9 GHz, which account for 86% of the Ka band (27–40 GHz) [3]. The DGS approach has been used to construct an array antenna for Radio Detection and Ranging (RADAR) applications in the Ka-Band frequency band [4]. For upcoming 5G devices running across 28 GHz and 38 GHz, a small, ultra-wideband, high-gain Multiple Input Multiple Output (MIMO) antenna is introduced. The substrate material used to design the exhibited antenna is Roger RT/Duroid 6002, which has a thickness of 1.52 mm. To increase impedance bandwidth and achieve ultra-wideband, the antenna is loaded with different stubs. The suggested design has dimensions of  $27 \times 27 \times 1.52$  mm<sup>3</sup> and consists of stubs with loaded rectangular patches. The various stubs are loaded to the antenna to improve impedance bandwidth

and obtain ultra-wideband. The resultant antenna operates over a broadband of 26.5–43.7 GHz, with a peak value of gain >8 dBi [5]. For 5G wireless networks, a small Multiple Input Multiple Output (MIMO) antenna specifically for the Ka-band has been created on the Rogers RT/Duroid 5880 substrate, which has dimensions of  $26 \times 25 \times 1.6 \text{ mm}^3$ . To provide polarisation variation in the 20–40 GHz frequency range, the antenna employs four P-shaped radiating patches in E-shaped slots [6]. For Ka-band operation, a four-element Multiple Input Multiple Output (MIMO) antenna has been developed. It has enhanced the bandwidth and improved the isolation to 30 dB by using the innovative decoupling structure. The antenna's maximum strength is 6.5 dBi, and its operational bandwidth is 24.1–30.9 GHz [7]. It is suggested that a small, arc-shaped antenna with a 28 GHz resonance be used for millimeter-wave applications in the 5G frequency range. The 1.3 mm radius of the circular monopole antenna is part of its design. On the radiating plane, an elliptical slot facilitates the attainment of a wider bandwidth resonance at 28 GHz. The antenna's average gain is about 4 dB across the whole impedance bandwidth, and its radiation efficiency is a respectable 89% [8]. For the three operational frequencies of 3.3 GHz, 4.5 GHz, and 5.8 GHz, a tri-band antenna has been constructed [9]. An LI-slotted patch antenna was suggested for 5G applications operating at 26.28 GHz and 28.54 GHz [10]. For 5G applications, the surface response approach is used in the design of the pi-slotted dual-band rectangular microstrip patch antenna. At 28 GHz and 38 GHz, the suggested antenna also provides gains of 6 dBi and 4.15 dBi, respectively. Also, over its whole impedance bandwidth, the VSWR is less than 2 [11]. At 28 GHz, a  $1 \times 4$  linear antenna array is suggested for 5G communication systems. The suggested array uses a  $1 \times 4$  T-power divider to supply power to four rectangular slotted antenna elements. In order to improve the total array gain and increase the radiation intensity, an Artificial Magnetic Conductor (AMC) layer is positioned beneath the array. Within the operational bands, the measured gain value of the suggested array design ranges from 11.8 dBi to 13.1 dBi, reaching 13.1 dBi at 28 GHz [12]. For 5G mobile networks, a low-profile antenna in the 26.75–30.31 GHz and 35.83–41.22 GHz frequency ranges was created. By co-centrally joining two planar hexagonal rings, the suggested antenna employs a meta-material-based construction that consists of a Split-Ring Resonator (SRR) and a Closed-Ring Resonator (CRR) [13]. For Ka band applications, a microstrip patch antenna with resonant frequencies of 29.87 GHz and 35.02 GHz was created [14]. For Ka-band applications, a rectangular patch antenna based on the utilization of several slots on the patch has been devised [15]. A coplanar waveguide-fed wideband meander line antenna has been introduced for Ka band applications. The proposed antenna has been simulated on HFSS using Rogers RO4003 as the substrate with dimensions  $22 \times 19 \times 1.52 \text{ mm}^3$ , which has a relative permittivity ( $\epsilon_r$ ) of 3.55. A ladder-shaped feed is used to give it a wide fractional bandwidth of 51.6% between 23 GHz and 39 GHz. At the central frequency of 29.11 GHz, the antenna displays a gain of 5.45 dB, while at 37.5 GHz,

it displays a peak gain of 7.1 dB [16]. An innovative tri-band antenna based on metamaterials for the 5G-C and Ka frequencies. The suggested antenna achieves three operational bands with decreased overall antenna dimensions by using a circular monopole loaded with a complementary split ring resonator, a rectangle patch with an E-shaped slot, and an inverted U-structured patch. The overall dimension of the proposed tri-band antenna is  $30 \times 22 \times 0.543 \text{ mm}^3$ , and the bandwidths measured are 9.04%, 14.14%, and 2.46% at 4.7 GHz, 28 GHz, and 39 GHz, respectively. It has also measured gain values of 2.5 dBi, 7.06 dBi, and 6.76 dB, respectively [17]. For Ka-band applications, a small CPW-fed monopole antenna based on the Artificial Magnetic Conductor (AMC) has been proposed. Using AMC with four stubs and a circular slot at 28 GHz improves the monopole antenna's radiation properties. In the frequency range of 25.76–35.86 GHz, the gain for this antenna is 8.76 dBi [18]. Patch antennas are made for dual bands, such as the S and C bands, which operate in the 2.53–7.707 GHz frequency range [19]. For 5G applications, Multiple Input Multiple Output (MIMO) antennas are planned to operate at 3.41 GHz with a gain of 4.2 dB [20]. The effect that the radiating conductor's thickness has on the antenna's gain is examined mathematically [21]. A small loaded microstrip patch antenna with an Artificial Magnetic Conductor (AMC) has been designed on the substrate dimensions of  $20 \times 20 \times 2.4 \text{ mm}^3$  in the frequency range of 28.4–36 GHz. The gain was increased from 3 dB to 5.80 dB by placing an Artificial Magnetic Conductor (AMC) array ( $8 \times 8$ ) layer between the radiating patch and ground. [22]. On the basis of the patch's slots and Defective Ground Structure (DGS), a wideband antenna was created for Ka-band applications [23]. A log-periodic  $1 \times 9$  antenna array configuration with a 9.25 dBi gain value has been developed for high-gain applications [24]. To provide 5.13 GHz and 11.63 GHz bandwidth at 28 GHz and 38 GHz, respectively, a  $2 \times 2$  Multiple Input Multiple Output (MIMO) was constructed on the substrate dimensions  $8.25 \times 9.69 \times 0.45 \text{ mm}^3$  [25]. For upcoming multi-band 5G wireless communication applications, a low-profile microstrip patch antenna fed by a tri-band microstrip line is recommended. The recommended antenna is printed on Rogers 5880 substrate of dimensions  $26 \times 16.5 \times 0.508 \text{ mm}^3$ . The recommended antenna design offered the gains of 5.67 dBi at 10 GHz, 9.33 dBi at 28 GHz, and 9.57 dBi at 38 GHz [26]. A symmetric four-element Multiple Input Multiple Output (MIMO) with inverted I-shaped slots and rectangular patches has been designed on the substrate dimensions of  $55 \times 110 \times 0.508 \text{ mm}^3$ . The proposed design provides gain values of 5.24 dBi and 4.34 dBi at 28 GHz and 38 GHz, respectively [27]. A planar circularly polarised Substrate Integrated Waveguide (SIW) stacked patch antenna array consisting of Four Sequential-Rotation (SR) subarrays is presented for Ka-band applications. The presented antenna provides a -10 dB impedance bandwidth of 29.6%, a 3 dB axial ratio bandwidth of 25.4%, and a peak gain of 20.32 dBi [28].

Various antennas for Ka-Band applications have been built by researchers using a variety of approaches found in the literature, such as decoupling structure, orthogonal

diversity, Artificial Magnetic Conductor (AMC) array, Defective Ground Structure (DGS), and different slots on the patch. An innovative 10-element array antenna design concept has been put up for Ka-band applications, particularly 5G communications. Furthermore, there is a good agreement between the measured and simulated findings.

Around the world, engineering firms, educational institutions, and learning technology use the Computer Simulation Technology (CST) studio suite, a collection of tools for developing, modelling, and improving electromagnetic systems. The Computer Aided Design (CAD) import tools and robust modelling environment in the Computer Simulation Technology (CST) studio suite assist the user in creating the necessary representative model of the system. The comprehensive technical approach of Computer Simulation Technical (CST) enables the verification of a simulation through the comparison of the output from numerous solvers, such as the time domain solver, within a single interface. This kind of cross-checking with the simulations increases trust in the simulation's correctness and aids engineers in modelling, analysing, and estimating measurement errors without recognising the electromagnetic component. The Computer Simulation Technology (CST) studio suite components have built-in optimisers that can be used to optimise a variety of factors, such as the excitation waveform, material properties, and model geometry.

An introduction and literature review, a suggested antenna design, findings and discussions, and a conclusion are the four sections that make up this paper. Using the inset feeding approach, a non-uniform structure with non-uniform spacings between the patches is employed as an array antenna for Ka-band applications. The primary objective of this study is to construct a single microstrip patch with inset feeding. Second, for Ka-Band frequencies ranging from 26 GHz to 40 GHz, the suggested antenna was built using simulation software before being assessed for several critical parameters, such as gain, reflection coefficient, and Voltage Standing Wave Ratio (VSWR). Third, important characteristics including gain, reflection coefficient, and Voltage Standing Wave Ratio (VSWR) have been experimentally tested and measured in the suggested antenna. Fourth, a developed antenna for use in Ka-Band applications has been completed, and the measurement results indicate that the proposed antenna is most appropriate for Ka-Band systems. The scope of the task has also been specified for the future.

## II. ANTENNA DESIGN

Based on the idea of an inset feeding mechanism, a wideband 10-element array antenna is constructed in two stages. A single inset-fed microstrip patch antenna was constructed as the initial phase. The second phase involves designing a wideband 10-element array antenna using the concept of a non-uniform structure with non-uniform spacing between the patches. Additionally, a broadband 10-element array antenna with a height of 0.757 mm and a loss tangent of 0.0009 is designed on the RT Duriod 31.3 × 10.37 × 0.787 mm<sup>3</sup> substrate. The substrate material is

RT Duriod 5880 with a dielectric constant of 2.2, as shown in Fig. 1. Once the substrate has been selected, the design equations are used to determine the patch antenna's dimensions. After constructing the patch antenna, the non-uniform sizes and spacings between the elements are adjusted to design a 10-element array antenna in a series-fed structure based on the concept of a non-uniform structure with non-uniform spacing between the patches.

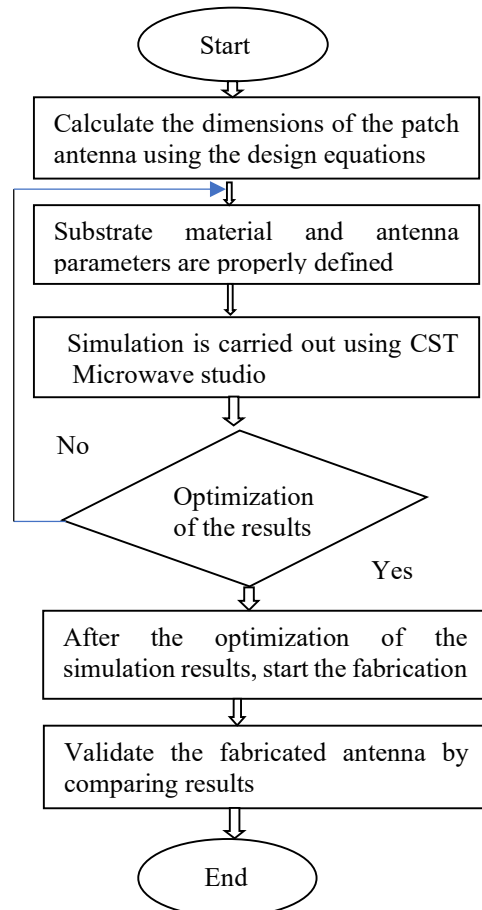


Fig. 1. Design flow chart.

Additionally, modelling is done to determine the key parameters after building a 10-element array antenna. Additionally, in order to attain ultra-wideband characteristics, parametric analysis is performed for the antenna array by applying multiple inter-element spacings and taking varied patch dimensions. Following simulation, a 10-element array antenna is constructed and subsequently measured. Finally, the simulated and measured parameters are compared to confirm that the suggested antenna can operate at Ka-band frequencies. There are two primary design steps along with the overall design flow.

### Step 1: Design of single inset-fed microstrip patch antenna.

In the first step, a single inset-fed microstrip patch antenna is designed based on the following equations [2].

$$W = \frac{c}{2f_r} \sqrt{\frac{2}{\epsilon_r + 1}} \quad (1)$$

“ $W$ ” in Eq. (1) stands for the patch’s width. The resonant frequency, input impedance, radiation pattern, and bandwidth of a microstrip patch antenna are all directly impacted by the patch’s width, making it an essential component. The antenna’s resonant frequency is mostly determined by the patch’s width; a broader patch resonates at a lower frequency, while a narrower patch resonates at a higher frequency. The antenna’s input impedance, which must match the feeding line for the best power transfer, can be controlled by varying the patch width. Sometimes expanding the patch width results in a greater bandwidth, which allows the antenna to function across a larger frequency range. The direction of the electromagnetic waves’ emission is influenced by the patch’s breadth, which also has an impact on the antenna’s radiation pattern.

$$\epsilon_{r_{eff}} = \frac{\epsilon_r + 1}{2} + \frac{\epsilon_r - 1}{2} \left( 1 + 12 \frac{h}{w} \right)^{-\frac{1}{2}} \quad (2)$$

In Eq. (2),  $\epsilon_{r_{eff}}$  represents the effective dielectric constant of the microstrip patch. The “effective dielectric constant” of a microstrip patch is important because it directly affects the antenna’s resonant frequency, which is essentially its operating frequency. It also plays a critical role in optimising the patch antenna’s size, gain, and bandwidth because it takes into account the fringing fields around the patch edges, which are influenced by the substrate material and its dielectric properties. A higher effective dielectric constant result in a smaller patch size for the same resonant frequency but may also restrict the antenna’s bandwidth. For the same operating frequency, a smaller patch size is possible with a higher effective dielectric constant. The effective dielectric constant, which is crucial for precise antenna design, considers the “fringing fields” that extend over the patch borders in addition to the dielectric constant of the substrate material. An antenna’s bandwidth is typically increased by selecting a substrate with a lower dielectric constant. Engineers carefully choose the substrate material when developing a microstrip patch antenna in order to attain the required effective dielectric constant for the best performance.

$$L_{eff} = \frac{c}{2f_r \sqrt{\epsilon_{r_{eff}}}} \quad (3)$$

In Eq. (3),  $L_{eff}$  represents the effective length of the patch. In order to accurately calculate the resonant frequency and radiation pattern in design calculations, it is essential to consider the “effective length” of a microstrip patch antenna. This is because it represents the electrically larger length of the patch due to fringing fields at its edges; in other words, it accounts for the “extra” electrical length caused by the fringing fields around the patch edges. Because the fringing fields extend over the patch’s actual boundaries, the antenna appears electrically larger than it actually is. The dielectric constant of the substrate material influences the effective length, which in turn influences the propagation of the electric fields around the patch. A microstrip patch antenna’s resonance frequency can be

precisely calculated by using the effective length instead of the physical length.

$$\Delta L = 0.421h \frac{(\epsilon_r + 0.3) \left( \frac{w}{h} + 0.264 \right)}{(\epsilon_r - 0.258) \left( \frac{w}{h} + 0.8 \right)} \quad (4)$$

In Eq. (4), ‘ $\Delta L$ ’ represents the additional length of the patch. In order to account for the “fringing fields” around the patch’s edges, ‘ $\Delta L$ ’ must be added to the physical patch length of a microstrip patch antenna. This effectively represents the effective length of the antenna as a result of these electric field extensions, and it is essential for precisely determining the antenna’s resonant frequency during design. The patch’s length is essentially increased by the “fringing field” created by the electric fields surrounding its boundaries, which extend just a little bit beyond its actual dimensions. Designers can determine the proper patch dimensions to attain the intended resonance frequency by taking the delta length into account. In order to estimate the effective length, delta length is frequently added to the physical patch length and is typically computed using parameters such as substrate thickness, dielectric constant, and patch width.

$$L = L_{eff} - 2\Delta L \quad (5)$$

“ $L$ ” stands for the patch’s length in Eq. (5). Because it directly affects the resonant frequency at which the antenna functions, the length of a microstrip patch is essential. This means that by varying the patch length, you may precisely regulate the frequency at which the antenna will emit electromagnetic waves most effectively. In essence, a longer patch means a lower resonance frequency, and vice versa, according to the idea that the patch length in the dielectric substrate material is around half the wavelength of the intended operating frequency. The most crucial element is that the patch length is the main factor determining the resonance frequency of the antenna; by varying this size, designers can customise the antenna for particular uses. A key idea in the design of microstrip antennas is that the patch’s length should be nearly half the wavelength of the operating frequency in the dielectric substrate material. The effective length is marginally more than the physical length because of fringing fields at the patch’s boundaries, which must be taken into account while doing design calculations.

Fig. 2 shows the single microstrip patch antenna that is designed based on the inset-feeding technique. This antenna has been used as the basis for the construction of a wideband 10-element microstrip patch antenna with variable size, and its dimensions are provided in Table I. The length and width of the patch antenna are indicated by the measurements  $L_p$  and  $W_p$ , much like in Fig. 2. Furthermore, the length and width of the feeding are indicated by  $L_f$  and  $W_f$ . As in Fig. 2,  $w_n$  represents the notch width, and  $y_p$  represents the length from the notch to the patch edge.

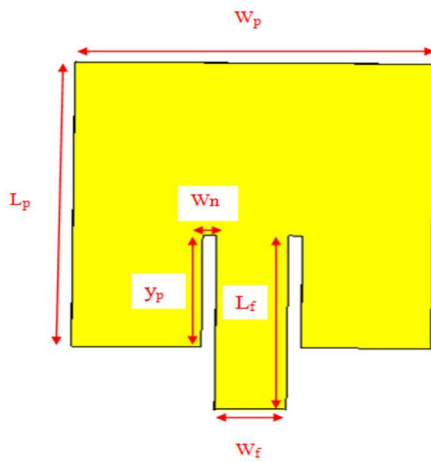


Fig. 2. Inset-fed microstrip patch antenna.

**Step 2: Design of 10-element non-uniform array antenna.**

The second step involves designing a wideband 10-element non-uniform array antenna with varying dimensions from the first to the tenth element.

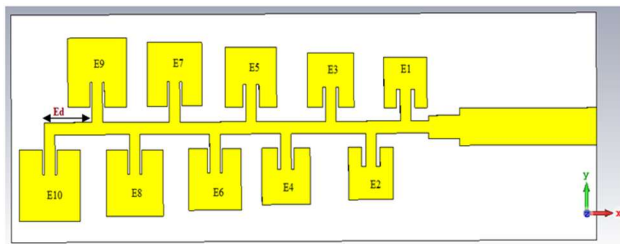


Fig. 3. Non-uniform 10 element array antenna.

Furthermore, there is space between the components. The non-uniform 10-element array antenna, which is based on the idea of a non-uniform structure with non-uniform spacing between the patches, is shown in Fig. 3. E1 through E10 are the 10 antennas or elements, as shown in Fig. 3. Furthermore, the distance between elements has been shifted from E1 to E10.

Table I is a tabulation of the non-uniform 10-element elements' dimensions. Table I lists the 10-element array antenna's measurements, including the patch's length and width as well as the feeding slot's length and width. Additionally, Table I shows that the elements are spaced apart.

TABLE I. DIMENSIONS OF THE PROPOSED ANTENNA

Element	$L_p=W_p$ (mm)	$Y_p$ (mm)	$W_n$ (mm)	$L_f$ (mm)	$W_f$ (mm)	$E_d$ (mm)
1	2.4	0.88	0.22	1.47	0.56	2.55
2	2.49	0.93	0.14	1.60	0.56	3.99
3	2.58	0.98	0.16	1.62	0.56	3.58
4	2.74	1.04	0.15	1.65	0.56	3.72
5	2.81	1.11	0.11	1.75	0.56	3.52
6	2.81	1.11	0.11	1.77	0.56	3.24
7	2.92	1.11	0.11	1.84	0.56	3.70
8	3.03	1.12	0.10	1.83	0.56	3.98
9	3.14	1.12	0.10	1.82	0.56	3.44
10	3.25	1.12	0.10	1.82	0.56	2.82

III. RESULTS AND DISCUSSIONS

Because of its wide bandwidth, which enables a single antenna to transmit on frequencies in numerous bands, the non-uniform structure with non-uniform spacing between the patches is frequently employed as a transmitting antenna in high-power shortwave broadcasting stations. Using up to ten elements, the non-uniform structure with non-uniform spacing between the patches design has been employed.

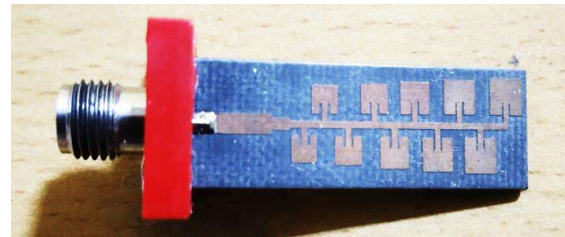


Fig. 4. Fabricated 10-element array antenna.

According to Fig. 4, the fabricated 10-element array antenna has a height of 0.757 mm and a loss tangent of 0.0009 based on the non-uniform structure with non-uniform spacing between the patches. It is developed on the RT Duriod  $31.3 \times 10.37 \times 0.787$  mm<sup>3</sup> substrate. Gain, Voltage Standing Wave Ratio (VSWR), and reflection coefficient of the manufactured antenna are all simulated.

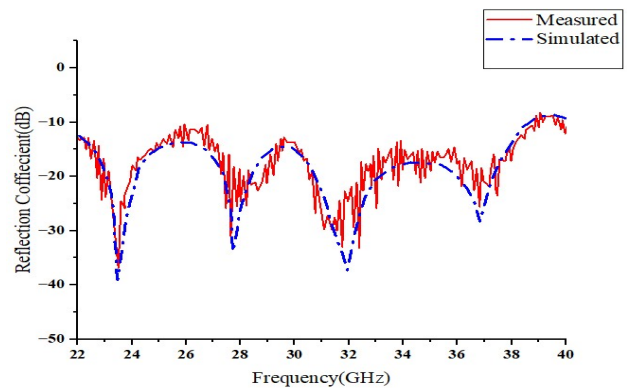


Fig. 5. Reflection coefficient.

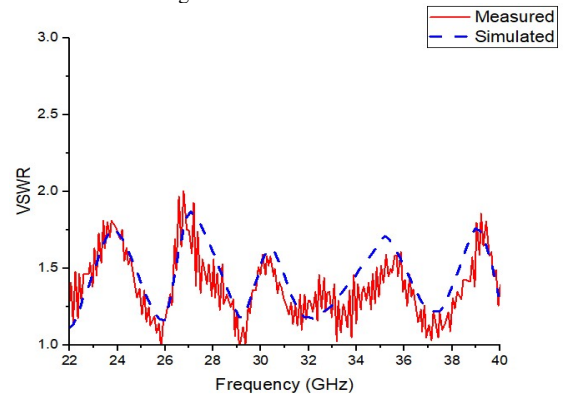


Fig. 6. VSWR.

The simulated and measured reflection coefficients of a 10-element array antenna are shown in Fig. 5. Both the measured and simulated reflection coefficients are less

than  $-10$  dB in the 22 GHz–40 GHz frequency range, as shown in Fig. 5. The reflection coefficient value is also suitable for Ka-band applications.

A 10-element array antenna’s measured and simulated VSWR is shown in Fig. 6. The simulated and measured VSWR values in the 22 GHz to 40 GHz frequency range are less than 2, as shown in Fig. 6. Additionally, for Ka-band applications, the VSWR value is acceptable.

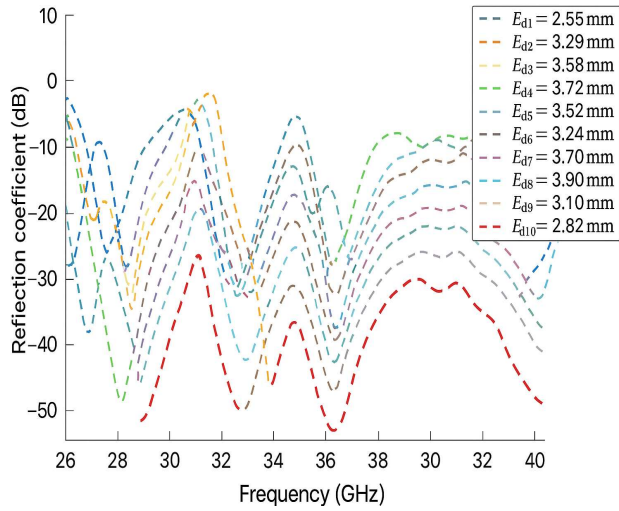


Fig. 7. Parametric analysis of reflection coefficient.

The parametric study of the reflection coefficient of the constructed 10-element array antenna for different elementary spacing lengths between the first and tenth elements is shown in Fig. 7. As shown in Fig. 7, the reflection coefficient in the 22 GHz–40 GHz frequency band is less than  $-10$  dB. Furthermore, for Ka-band applications, the reflection coefficient value is appropriate.

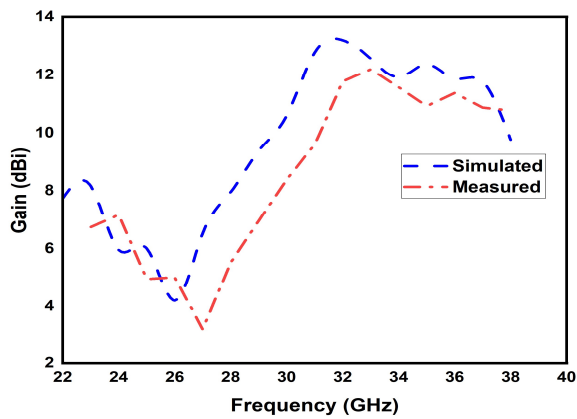


Fig. 8. Gain.

The measured and simulated gains of a 10-element array antenna are shown in Fig. 8. The measured gain is 12.2 dBi, while the simulated gain is 13.2 dBi, as shown in Fig. 8. Furthermore, in the frequency range of 22 GHz to 40 GHz, the simulated and measured gain values nearly match. Furthermore, the gain value is quite high and suitable for Ka-band applications.

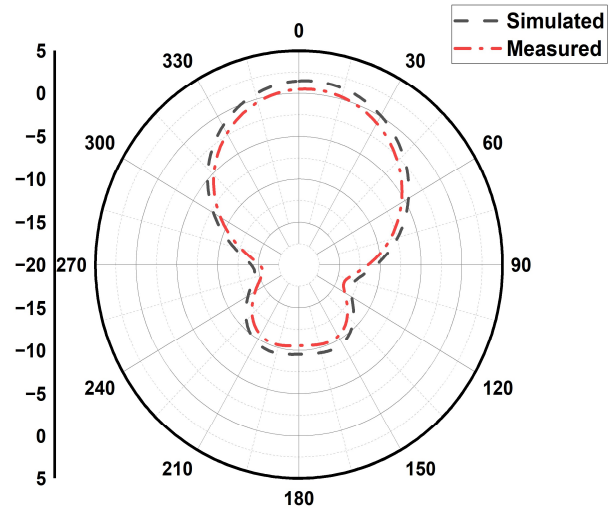


Fig. 9. E-plane pattern at 23.4GHz.

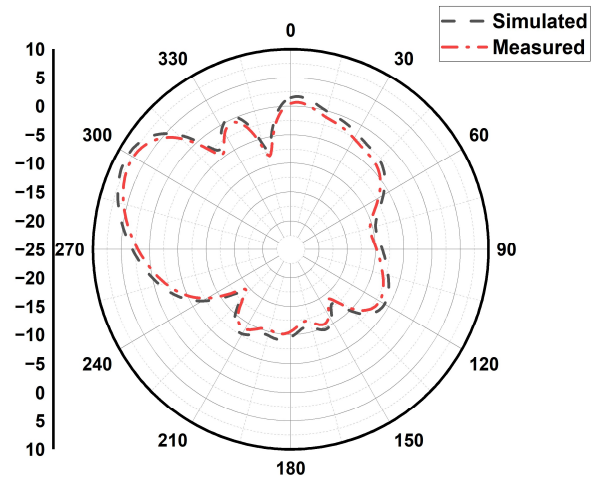


Fig. 10. H-plane pattern at 23.4 GHz

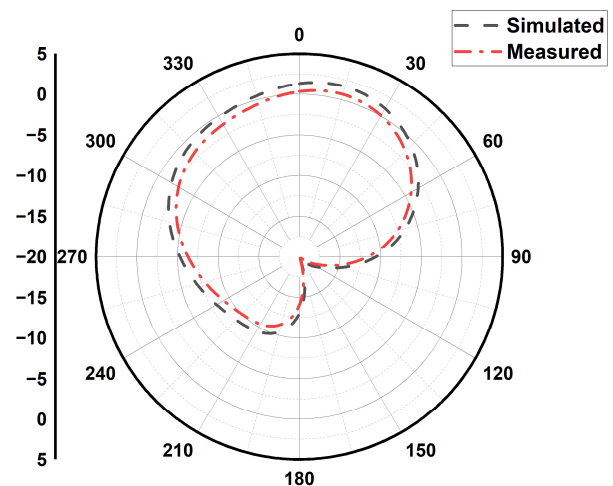


Fig. 11. E-plane pattern at 27.6 GHz.

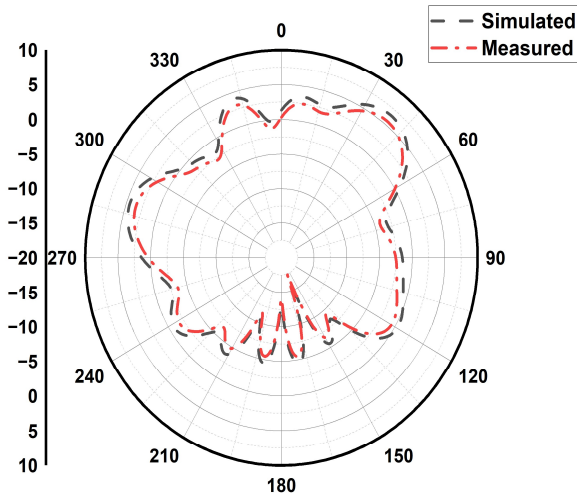


Fig. 12. H-plane pattern at 27.6 GHz.

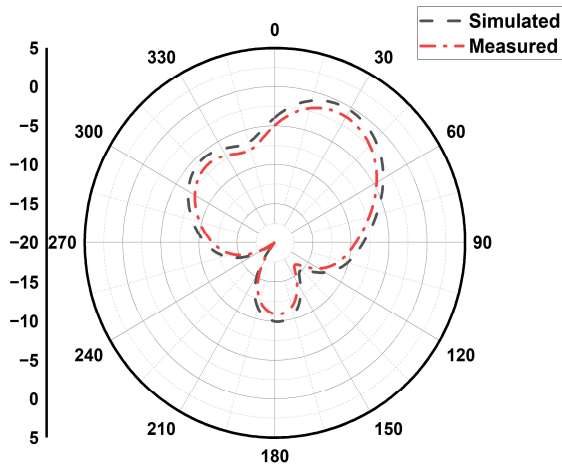


Fig. 13. E-plane pattern at 31.5 GHz.

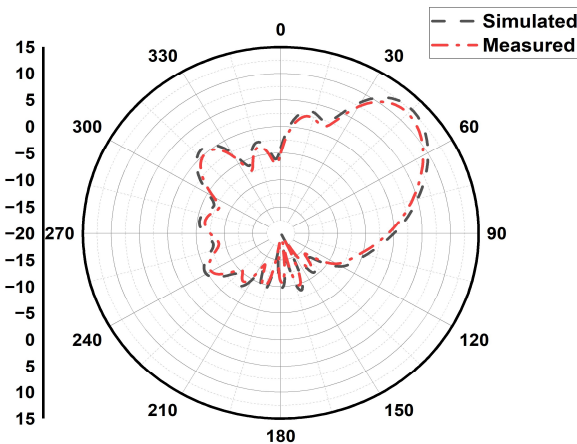


Fig. 14. H-plane pattern at 31.5 GHz.

on these H-plane patterns, it can be concluded that all of the aforementioned frequencies experienced the highest radiation levels. Furthermore, there is a strong agreement between the measured and simulated E-plane patterns. Additionally, there is a good agreement between the measured and simulated H-plane patterns. The Ka-band applications can use any of these patterns. In general, an electric field exists in the E-plane, while a magnetic field arises in the H-plane. An antenna's radiated power in a particular direction is indicated by the E-plane, and its radiated power in all directions is indicated by the H-plane.

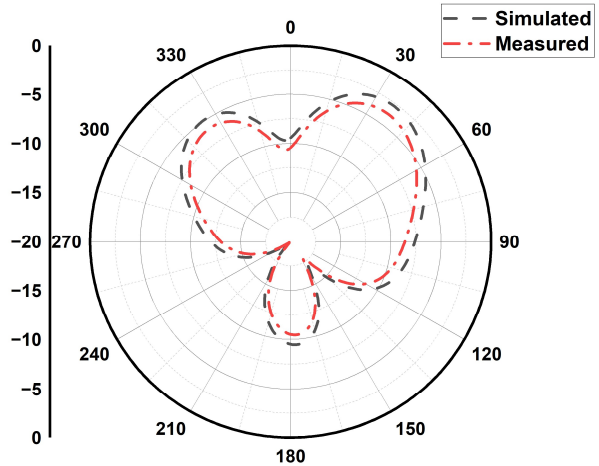


Fig. 15. E-plane pattern at 37.1 GHz.

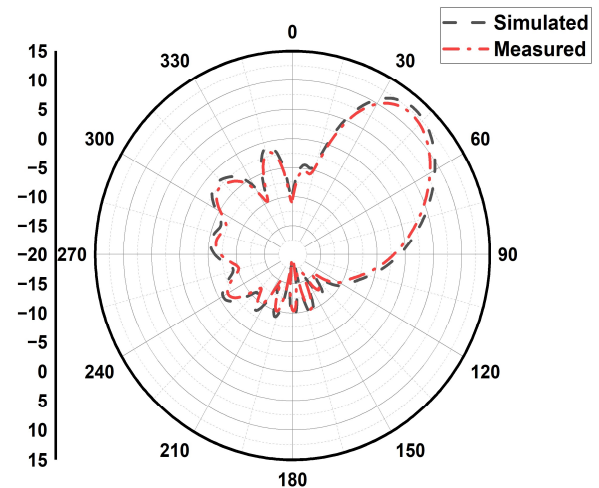


Fig. 16. H-plane pattern at 37.1 GHz.

TABLE II. COMPARISON OF SIMULATED AND MEASURED VALUES

S.No	Parameter	Simulated value	Measured value
1	Operating Frequency range	22 GHz–38.75 GHz	22 GHz – 38.75 GHz
2	Reflection coefficient	-39.06 dB	-36.8 dB
3	Bandwidth	16.37 GHz	16.75 GHz
4	VSWR	< 2	< 2
5	Peak gain	13.2 dBi	12.2 dBi

Figs. 9–15 show that E-plane patterns at several frequencies, including 23.4 GHz, 27.6 GHz, 31.5 GHz, and 37.1 GHz, were simulated and measured. It may be inferred from these E-plane patterns that all of the frequencies listed above experienced the highest radiation levels. Similarly, Figs. 10–14 and Fig. 16 show that H-plane patterns at several frequencies, including 23.4 GHz, 27.6 GHz, 31.5 GHz, and 37.1 GHz, were simulated and measured. Based

Comparing simulated and measured results in the 22 GHz–38.75 GHz frequency range is shown in Table II. The simulated and measured reflection coefficient values are both less than  $-10$  dB in this frequency range. As shown in Table II, in the frequency range of 22 GHz to 38.75 GHz, the maximum bandwidth of 16.37 GHz was attained. Additionally, Voltage Standing Wave Ratio (VSWR) of less than two is attained. Additionally, the frequency range described above yielded the largest gain, 12.2 dBi. It is observed from the measured values that the suggested antenna is appropriate for Ka-Band applications.

Our findings are contrasted with the published works in the literature in Table III. Our recommended antenna has a higher gain and bandwidth and also a superior design than the antennas presented in Refs. [5, 16, 17, 22, 25, 26, 27]. Despite having a larger bandwidth and gain than our suggested antenna, Hussain *et al.* [6] highbred dimension. It is determined that our suggested antenna is suitable for Ka-band applications, particularly for 5G communications, after comparing it with earlier research studies.

TABLE III. COMPARISON WITH PREVIOUS WORKS

Ref	Size (mm <sup>3</sup> )	No of elements	Bandwidth (GHz)	Gain (dBi)	Band	Operating frequency range
[5]	$27 \times 27 \times 1.52$	4	15.2	6	Ka	26.5–41.7 GHz
[6]	$26 \times 25 \times 1.6$	4	20	17.6	Ka	20–40 GHz
[16]	$22 \times 19 \times 1.52$	1	16	7.1	Ka	23–39 GHz
[17]	$30 \times 22 \times 0.543$	1	11	6.76	Ka	28–39 GHz
[22]	$20 \times 20 \times 2.4$	8	7.6	5.8	Ka	28.4–36GHz
[25]	$8.25 \times 9.69 \times 0.45$	2	10	8.31	Ka	28–38 GHz
[26]	$20 \times 16.5 \times 0.508$	1	0.101	9.57	Ka	10, 27.5, $\times$ 37.8GHz
[27]	$55 \times 110 \times 0.508$	4	10	$7.95 \times 8.27$	Ka	$28.044 \times 38.04$ GHz
Proposed work	$31.3 \times 10.37 \times 0.787$	10	16.75	12.2	Ka	22–38.75GHz

#### IV. CONCLUSION

This study proposes a 10-element series-fed array antenna with an irregular shape and unequal spacing for Ka-Band (26 GHz–40 GHz) applications. It is based on the non-uniform structure with non-uniform spacing between the patches. Essential characteristics, including gain, Voltage Standing Wave Ratio (VSWR), and reflection coefficient, are simulated and designed into the suggested antenna. The developed antenna is then manufactured and tested for the same crucial characteristics following simulation. The suggested antenna for Ka-band frequencies has been validated by comparing the measured and simulated parameters after measurement. Following the comparison, the frequency range of 22 GHz to 38.75 GHz has a broad bandwidth of 16.75 GHz, a reflection coefficient  $< -10$ dB, Voltage Standing Wave Ratio (VSWR)  $< 2$ , and a peak gain of 12.2 dBi. Finally, the proposed antenna has the advantage of being low-cost and lightweight, which is especially helpful for millimetre wave and 5G applications.

Future goals for this work include building an antenna for wideband, 5G, and multi-band applications by expanding the number of patches in terms of feeding techniques, material selection, and uniform and non-uniform techniques. If the mutual coupling between the patches is decreased and the number of patches is increased, the suggested antenna can be utilised for 6G applications. If a zigzag pattern is chosen for the number of patches, the suggested antenna will change to a log-periodic antenna. Lastly, the suggested antenna works well for high-gain applications like 5G, 6G, and mobile satellite.

#### CONFLICT OF INTEREST

The authors declare no conflict of interest.

#### AUTHOR CONTRIBUTIONS

Pavada Santosh and P. Ramesh have collected the data and designed the antenna in the simulation software to get simulation results; Chitambara Rao Karedla and K. S. Chakradhar have analyzed the simulation results and also fabricated the designed antenna; M. Lakshmunaidu and Harihara Santosh Dadi have taken the measurement results for a fabricated antenna; Finally, all the authors have compared the simulation and measured results for the validation of the designed antenna and approved the final version of the paper.

#### REFERENCES

- [1] K. C. Rao, D. Nataraj, K. S. Chakradhar, G. V. Ujwala, M. Lakshmunaidu, and H. S. Dadi, "Design of a compact millimeter wave antenna for 5G applications based on meta surface luneburg lens," *Engineering, Technology and Applied Science Research*, vol. 15, no. 2, pp. 20722–20728, 2005.
- [2] S. Rana and O. Faruq, "Design and analysis of Ka-band microstrip patch antenna for wireless applications," *Indonesian Journal of Electrical Engineering and Computer Science*, vol. 31, no. 2, pp. 802–809, 2023.
- [3] R. K. Mistri, S. K. Mahto, A. K. Singh, R. Sinha, A. J. A. A. Gburi, T. A. H. Alghamdi, and M. Alathbah, "Quad element MIMO antenna for C, X, Ku, and Ka-band applications," *Sensors*, 2023.
- [4] S. Aourik, A. Errkik, J. Zbitou, R. Mandry, and A. L. Sassi, "Millimetre microstrip antennas for radar applications in the Ka-band," *IGI Global*, p. 76, 2023.
- [5] S. A. Hussain, F. Taher, M. S. Alzaidi, I. Hussain, R. M. Ghoneim, F. A. Sree, and A. L. bakhsh, "Wideband, high-gain, and compact four-port MIMO antenna for future 5G devices operating over Ka-band spectrum," *Spectrum. Appl. Sci.*, vol. 13, 2023.

- [6] P. Tiwari, V. Gahlaut, U. N. Mishra, A. Shastri, and M. Kaushik, "Polarization diversity configuration of millimeter wave MIMO antenna for Ka-band application in 5G wireless networks," *Journal of Electromagnetic Waves and Applications*, vol. 38, pp. 486–507, no. 4, 2024.
- [7] B. G. P. Shariff, A. A. Naik, T. Ali, P. R. Mane, R. M. David, S. Pathan, and J. Anguera, "High-isolation wide-band four-element MIMO antenna covering Ka-band for 5G wireless applications," *IEEE Access*, pp. 123030–123046, 2023.
- [8] P. Kumar *et al.*, "An ultra-compact 28 GHz arc-shaped millimeter-wave antenna for 5G application," *Micromachines*, vol. 14, no. 1, 2023.
- [9] N. Q. A. Alshaikhli, M. A. Neamah, and M. I. A. Nouman, "Design of triband antenna for telecommunications and network applications," *Bulletin of Electrical Engineering and Informatics*, vol. 11, no. 2, pp. 1084–1090, Apr. 2022.
- [10] M. Nahas, "Design of a high-gain dual-band LI-slotted microstrip patch antenna for 5G mobile communication systems," *Journal of Radiation Research and Applied Sciences*, vol. 15, no. 4, 100483, Dec. 2022.
- [11] L. G. Ayalew and F. M. Asmare, "Design and optimization of pi-slotted dual-band rectangular microstrip patch antenna using surface response methodology for 5G applications," *Heliyon*, vol. 8, no. 12, e12030, Dec. 2022.
- [12] A. A. Ibrahim *et al.*, "Slotted antenna array with enhanced radiation characteristics for 5G 28 GHz communications," *Electronics*, vol. 11, 2664, 2022.
- [13] H. Ullah *et al.*, "A compact low-profile antenna for millimeter-wave 5G mobile phones," *Electronics*, vol. 11, no. 32, 2022.
- [14] D. Choudary, D. Singh, and B. Mohapatra, "Design of microstrip patch antenna for Ka-band (26.5–40 GHz) applications," *Materials Today*, vol. 45, 2021.
- [15] V. Sharma and A. Rawat, "Compact design of Ka-Band antenna for 5G applications," in *Proc. 2021 3rd International Conference on Signal Processing and Communication (ICPSC)*, 2021, vol. 15.
- [16] M. Gupta, A. Kumar, A. Dixit, and A. Kumar, "Wide-band meander line antenna for Ka band application," *Springer Nature*, pp. 133–139, 2021.
- [17] R. Ruchi and M. V. Kartikeyan, "Metamaterial-inspired tri-band antenna for 5G-C and Ka band applications," *Microwave and optical Technology Letters*, vol. 63, no. 9, 2021.
- [18] A. Kumar, A. Dixit, A. Kumar, and A. Kumar, "AMC-loaded compact CPW-Fed monopole antenna for Ka-band applications," *Springer Nature*, pp. 331–337, 2021.
- [19] K. Mazen, A. Emran, A. S. Shalaby, and A. Yahya, "Design of multi-band microstrip patch antennas for mid-band 5G wireless communication," *International Journal of Advanced Computer Science and Applications*, vol. 12, no. 5, pp. 459–469, 2021. doi: 10.14569/IJACSA.2021.0120557
- [20] S. Murugan, "Compact MIMO shorted microstrip antenna for 5G applications," *International Journal of Wireless and Microwave Technologies*, vol. 11, no. 1, pp. 22–27, Feb. 2021.
- [21] A. S. B. Mohammed *et al.*, "Mathematical model on the effects of conductor thickness on the centre frequency at 28 GHz for the performance of microstrip patch antenna using air substrate for 5G application," *Alexandria Engineering Journal*, vol. 60, no. 6, pp. 5265–5273, Dec. 2021. doi: 10.1016/j.aej.2021.04.050
- [22] K. Belabbas, D. Khedrouche, and A. Hocini, "Artificial magnetic conductor-based millimetre wave microstrip patch antenna for gain enhancement," *Journal of Telecommunications and Information Technology*, vol. 1, 2021.
- [23] A. R. Sabek, A. A. Ibrahim, and W. A. Ali, "Dual-band millimetre wave microstrip patch antenna with Stub Resonators for 28/38 GHz applications," *Journal of Physics: Conference Series*, vol. 2128, no. 1, 012006, Dec. 2021. doi: 10.1088/1742-6596/2128/1/012006
- [24] T. Varum, J. Caiado, and J. N. Matos, "Compact ultra-wideband series-feed microstrip antenna arrays for IoT communications," *Applied Sciences*, vol. 11, no. 14, 6267, July 2021.
- [25] M. L. Hakim, M. J. Uddin, and M. J. Hoque, "28/38 GHz dual-band microstrip patch antenna with DGS and stub-slot configurations and its 2x2 MIMO antenna design for 5G wireless communication," in *Proc. IEEE Symposium*, 2020, pp. 56–59. doi: 10.1109/TENSYMP50017.2020.9230601
- [26] A. Abdelaziz and E. K. I. Hamad, "Design of a compact high gain microstrip patch antenna for Tri-Band 5G wireless communication," *Frequenz*, vol. 73, no. 1–2, pp. 45–52, Jan. 2019. doi: 10.1515/freq-2018-0058
- [27] H. M. Marzouk, M. I. Ahmed, and A. A. Shaaan, "Novel dual-band 28/38 GHz MIMO antennas for 5G mobile applications," *Progress in Electromagnetics Research C*, vol. 93, pp. 103–117, 2019. doi: 10.2528/PIERC19032303
- [28] H. Xu *et al.*, "Planar wideband circularly polarized cavity-backed stacked patch antenna array for millimeter-wave applications," *IEEE Transactions on Antennas and Propagation*, vol. 66, no. 10, pp. 5170–5179, Oct. 2018.

Copyright © 2025 by the authors. This is an open access article distributed under the Creative Commons Attribution License which permits unrestricted use, distribution, and reproduction in any medium, provided the original work is properly cited ([CC BY 4.0](https://creativecommons.org/licenses/by/4.0/)).